

550 (Jasco) equipped with an integrating sphere attachment ISV-470 (Jasco) for diffuse-reflectance measurements. Measurements were made at 290 K in the wavelength range between 280 and 650 nm. UV-vis absorbance for all the compounds was obtained by the transformation based on the Kubelka–Munk equation.

3. Results

3.1. Ethanol photo-oxidation kinetics with UV-vis illumination

The time course of photo-oxidation reaction for ethanol (initial pressure 1.33 kPa) was depicted in Fig. 1 on mesoporous V + TiO₂ catalysts. Major products were acetaldehyde, water,

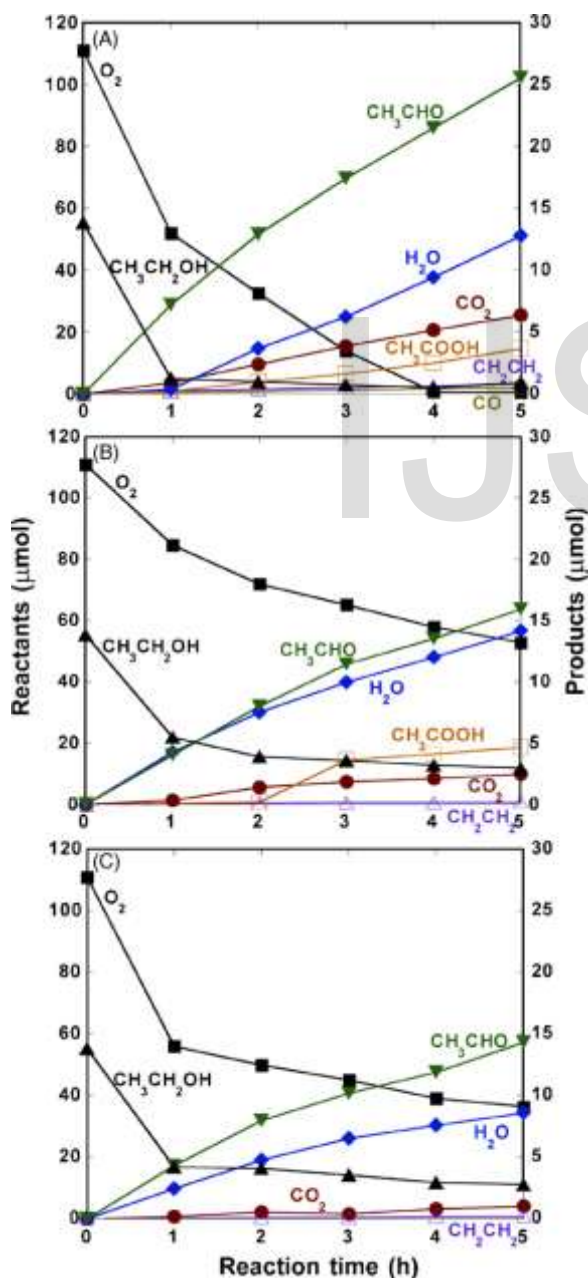


Fig. 1. Ethanol oxidation reaction as a function of time under the illumination of UV-vis light on mesoporous V + TiO₂ catalysts. Measured at 290 K. Ethanol (1.33 kPa) and O₂ (2.67 kPa) were introduced in closed circulating glass system (132 ml). (A) Mesoporous TiO₂. (B) Mesoporous V-TiO₂ (3.0 wt% V). (C) Impregnated V/mesoporous TiO₂ (3.0 wt% V).

carbon dioxide, and acetic acid on mesoporous TiO₂ (Fig. 1A) [34]. Because the ratio of formation rates for acetaldehyde and water was 2.2 (Table 1A), dehydration and dehydrogenation reactions for ethanol proceeded with comparable rates. Further photo-oxidized products acetic acid and carbon dioxide were minor. The formations of ethene and carbon monoxide were negligible.

In the photo-oxidation over mesoporous V-TiO₂ (3.0 wt% V), acetaldehyde and water were produced with essentially the same rates (Fig. 1B). Thus, ethanol dehydration proceeded predominantly in the presence of vanadium in the TiO₂ matrix [29]. Aceti

acid and carbon dioxide produced later than the induction period of 1–2 h because they were secondary or multiple-step products. For the impregnated V/mesoporous TiO₂ catalyst, the ratio of acetaldehyde and water formation rates was 1.8 (Fig. 1C and Table 1A). Thus, ethanol dehydration and dehydrogenation reactions proceeded with the rate ratio 1.3. Minor products were carbon dioxide and ethene. Compared to reactions on mesoporous TiO₂ and mesoporous V-TiO₂ (Fig. 1A and B), no acetic acid was found over impregnated V/mesoporous TiO₂.

The kinetics of ethanol photo-oxidation on V + TiO₂ (P-25) catalysts were summarized in Fig. 2 and Table 1A. On TiO₂ (P-25), major products were acetaldehyde and water, however, the formation rates were not constant (Fig. 2A) compared to the kinetics on mesoporous V + TiO₂ catalysts. The time course change for water formation was not monotonous. It was first deactivated and reactivated at 3 h. When vanadium was impregnated on TiO₂ (P-25) (Fig. 2B), the catalysis was suppressed compared to pure TiO₂ (P-25). Acetaldehyde was essentially the only one product via the ethanol dehydrogenation. The ethanol amount even increased in first 1 h in Fig. 2B. On vanadium-doped TiO₂ formic acid formation was reported [34], and in our Porapak-Q column formic acid and ethanol were not separated. Thus, the initial apparent increase of ethanol may be catalytic formation of formic acid.

In summary, under the illumination of UV-vis light, the ethanol dehydration rates followed the order (Table 1A)

$$\text{TiO}_2 \text{ mesoporous V TiO}_2 > \text{mesoporous TiO}_2 > \text{V=mesoporous TiO}_2 \quad \text{V=TiO}_2 \quad (1)$$

Ethanol dehydrogenation rates assumed based on the difference of acetaldehyde and water formation rates followed the order

$$\text{mesoporous TiO}_2 > \text{V=TiO}_2 > \text{V=mesoporous TiO}_2 > \text{TiO}_2 \text{ mesoporous V TiO}_2 \quad (2)$$

Table 1
Products formation rates in the ethanol photo-oxidation over various V + TiO₂ catalysts illuminated with UV + visible light (A) and visible light only (B)^a

	Formation rates (mmol h ⁻¹ g _{cat} ⁻¹)						
	MeCHO	H ₂ O	MeCO ₂ H	CO	CO ₂	C ₂ H ₄	S ^f
(A) UV + visible							
Mesoporous TiO ₂	72	33 ^c	11 ^c	0.85	14 ^c	1.3	92
Mesoporous V-TiO ₂ ^b	42	44	35 ^c	0	8.8 ^c	0.2	82
V/mesoporous TiO ₂ ^b	43	24	0	0	2.1 ^c	0.3	44
TiO ₂ (P-25)	61	50 ^d	0	0.3	6.4	0	64
V/TiO ₂ ^b	28	0	0	0	0.1	0	28
(B) Visible only							
Mesoporous TiO ₂	2.3	16 ^c	0	0	0.3 ^c	0	2.5
Mesoporous V-TiO ₂ ^b	23	212(16 ^e)	0	0	0.3 ^c	0	23
V/mesoporous TiO ₂ ^b	11	141(15 ^e)	0	0	0.2 ^c	0	11
TiO ₂ (P-25)	19	4.9 ^c	0	0	0.2 ^c	0	19
V/TiO ₂ ^b	18	0	0	0	0.9 ^c	0	18

^a Initial reactants: CH₃CH₂OH (55 mmol) and O₂ (110 mmol).

^b 3.0 wt% V.

^c Constant rates later than the induction period.

^d Serious deactivation observed.

^e Constant rate later than initial faster rate.

^f The summation of formation rates on the basis of carbon. The formation rates of CO and CO₂ were multiplied with a half in the summation.

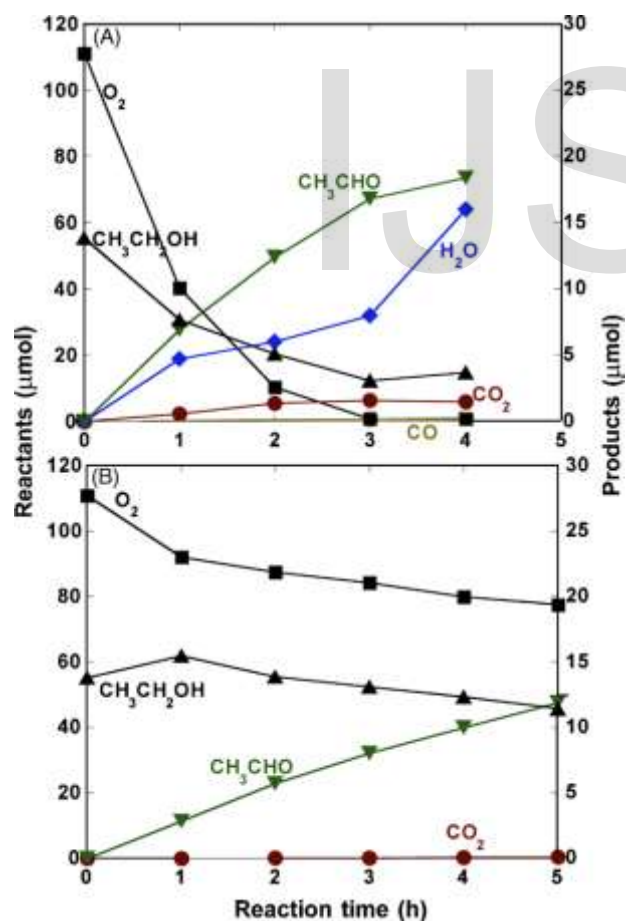


Fig. 2. Ethanol oxidation reaction as a function of time under the illumination of UV-vis light on conventional V + TiO₂ (P-25) catalysts. Reaction conditions were the same as noted in the caption for Fig. 1. (A) TiO₂ (P-25). (B) Impregnated V/TiO₂ (3.0 wt% V).

Acetic acid (and carbon dioxide) formation rates followed the order

$$\text{mesoporous V-TiO}_2 > \text{mesoporous TiO}_2 > \text{V-TiO}_2 > \text{V/mesoporous TiO}_2 \quad (3)$$

Ethanol photo-oxidation was reported on anatase TiO₂ and platinum-modified one [7]. The addition of Pt enabled catalytic formation of acetic acid similar to over mesoporous [V-]TiO₂ (Table 1A).

3.2. Ethanol photo-oxidation kinetics with visible light only illumination

The ethanol photo-oxidation results on mesoporous V + TiO₂ with visible light only illumination were depicted in Fig. 3 and the formation rates were summarized in Table 1B. The mesoporous TiO₂ catalyst was fairly inactive compared to the case illuminated with UV + visible light (Figs. 3A and 1A). Water was formed in addition to negligible acetaldehyde and carbon dioxide. Because the water evolving rate was greater than that of acetaldehyde by 7.0 times and ethanol in gas phase significantly decreased in the first 1 h, formed acetaldehyde may be trapped in mesopores of the TiO₂.

For mesoporous V-TiO₂ catalyst (3.0 wt% V), water was formed in first 1 h faster than for mesoporous TiO₂ by 13 times (Fig. 3B), even faster than in the measurement with UV + visible light illumination (Fig. 1B) by 4.8 times. Later than 1 h, the formation rates of water and acetaldehyde became constant and comparable (16 and 23 mmol h⁻¹ g_{cat}⁻¹, respectively, Table 1B). Minor product was carbon dioxide. The kinetic result for impregnated V/mesoporous TiO₂ (Fig. 3C) was qualitatively similar to that for mesoporous V-TiO₂ (Fig. 3B). Initial faster evolution of water was again observed in first 1 h and then water and acetaldehyde were constantly produced (15 and 11 mmol h⁻¹ g_{cat}⁻¹, respectively). The constant formation rates decreased to 94 and 48%, respectively, of corresponding rates for mesoporous V-TiO₂ (Table 1B).

proceeded predominantly at the rate between 18 and 19 mmol h⁻¹ g_{cat}⁻¹ both on TiO₂ (P-25) and impregnated V/TiO₂ (Fig. 4A and B). The time course results were quantitatively the same on the two catalysts. Negligible carbon dioxide and water (at 5 h) formations were observed on impregnated V/TiO₂ and TiO₂ (P-25), respectively. As mentioned above under UV-vis light (Fig. 2B), the apparent increase of ethanol in first 1 h may be the contribution of produced formic acid [34].

In summary, under the illumination of visible light only, the ethanol dehydration rates followed the order (Table 1B)

$$\begin{aligned} \text{mesoporous V-TiO}_2 > \text{V-mesoporous TiO}_2 \\ \text{mesoporous TiO}_2 > \text{TiO}_2 > \text{V-TiO}_2 \end{aligned} \quad (4)$$

Ethanol dehydrogenation rates followed the order

$$\begin{aligned} \text{V-TiO}_2 > \text{TiO}_2 \quad \text{mesoporous V-TiO}_2 > \text{mesoporous} \\ \text{TiO}_2 \quad \text{V-mesoporous TiO}_2 \end{aligned} \quad (5)$$

No acetic acid and negligible carbon dioxide were formed on all V + TiO₂ catalysts under the illumination of visible light only. Under dark conditions at room temperature, no reaction proceeded in ethanol and O₂ over Pt-doped TiO₂ catalyst [7].

3.3. Diffuse-reflectance UV-vis absorption spectra for V-TiO₂ catalysts

UV-vis spectra were measured for V + TiO₂ catalysts in diffuse-reflectance mode. In comparison to the absorption data for TiO₂ (P-25), the absorption was extended to the higher

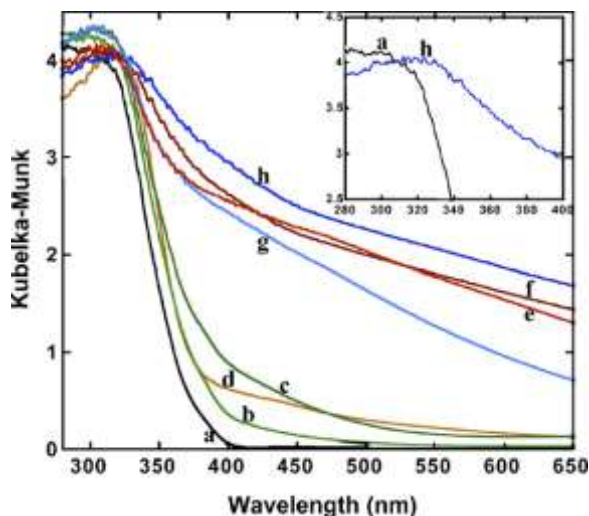


Fig. 5. Diffuse-reflectance UV-vis absorption spectra for TiO₂ (P-25) (a), impregnated V/TiO₂ (P-25) (1.0 and 3.0 wt% V) (b and c, respectively), mesoporous TiO₂ (d), mesoporous V-TiO₂ (1.0 and 3.0 wt% V) (e and f, respectively), and impregnated V/mesoporous TiO₂ (1.0 and 3.0 wt% V) (g and h, respectively). (Inset) Expanded data in the region between 280 and 400 nm for TiO₂ (P-25) (a) and V/mesoporous TiO₂ (3.0 wt% V) (h).

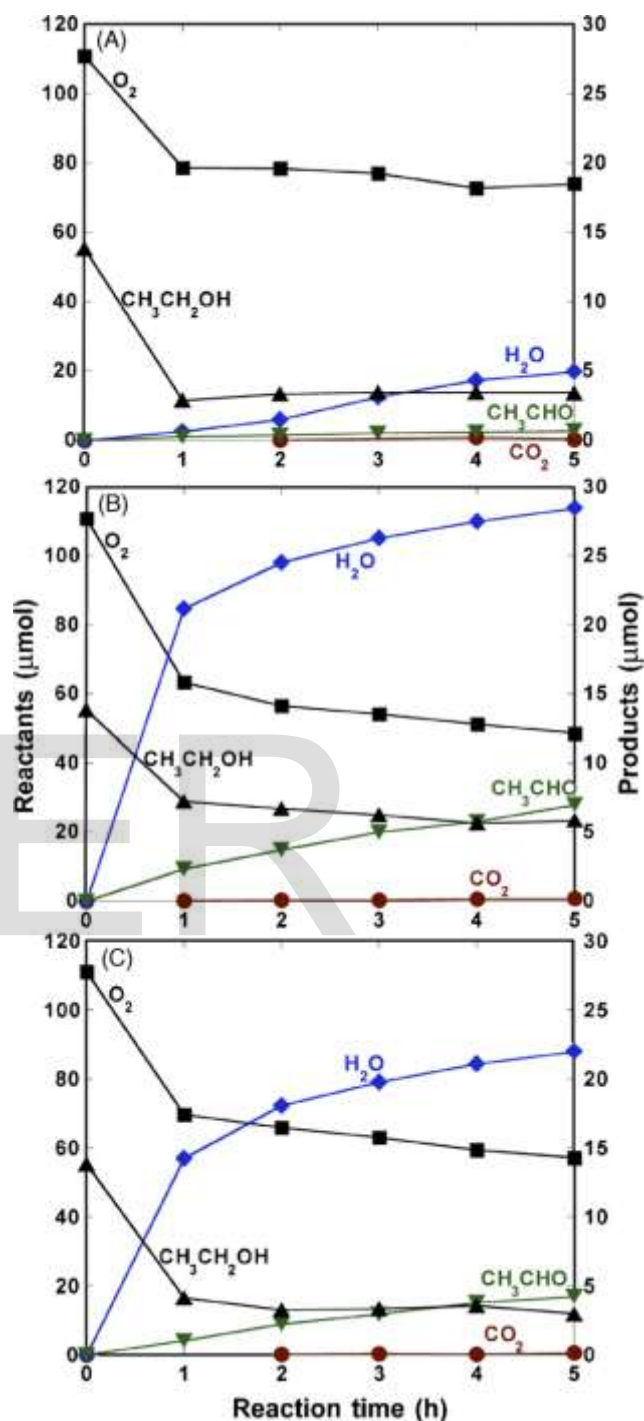


Fig. 3. Ethanol oxidation reaction as a function of time under the illumination of visible light only on mesoporous V + TiO₂ catalysts. Reaction conditions were the same as noted in the caption for Fig. 1. (A) Mesoporous TiO₂. (B) Mesoporous V-TiO₂ (3.0 wt% V). (C) Impregnated V/mesoporous TiO₂ (3.0 wt% V).

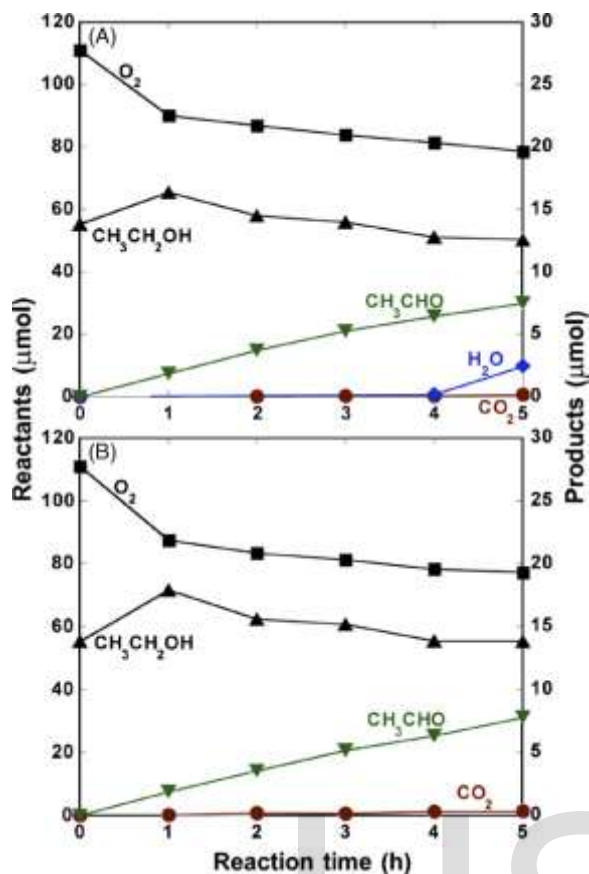


Fig. 4. Ethanol oxidation reaction as a function of time under the illumination of visible light only on conventional V + TiO₂ (P-25) catalysts. Reaction conditions were the same as noted in the caption for Fig. 1. (A) TiO₂ (P-25). (B) Impregnated V/TiO₂ (3.0 wt% V).

wavelength side when 1.0–3.0 wt% of V was impregnated (Fig. 5a–c) [4,8]. The extension toward visible light side was more enhanced for mesoporous TiO₂-based catalysts. Similar to the vanadium impregnation with TiO₂ (P-25), the V impregnation with mesoporous TiO₂ progressively extended the light absorption toward visible light region (Fig. 5g and h). In contrast, the extent of extension was independent to the V contents in catalysts for mesoporous V–TiO₂ between 1.0 and 3.0 wt% of V (Fig. 5e and f, respectively). The extent of extension toward visible light region was in the order

$$\begin{aligned} & \text{V=mesoporous TiO}_2 \delta 3:0\% \text{P} > \text{mesoporous V} \\ & \text{TiO}_2 \delta 1:0 \quad 3:0\% \text{P} > \text{V=mesoporous TiO}_2 \delta 1:0\% \text{P} \\ & > \text{V=TiO}_2 \delta 3:0\% \text{P} > \text{mesoporous TiO}_2 > \text{V=TiO}_2 \delta 1:0\% \text{P} \\ & > \text{TiO}_2 \delta \text{P-25} \end{aligned} \quad (6)$$

4. Discussion

Under the illumination of UV + visible light, total formation rates on carbon basis were in the order (Table 1)

$$\begin{aligned} & \text{mesoporous TiO}_2 > \text{mesoporous V} \quad \text{TiO}_2 > \text{TiO}_2 > \\ & \text{V=mesoporous TiO}_2 > \text{V=TiO}_2 \end{aligned} \quad (7)$$

As a general trend, mesoporous TiO₂-based catalysts were superior to anatase TiO₂-based catalysts (Table 1A). Various

kinds of specific photocatalysis under the illumination of light > 320 nm was reported using mesoporous TiO₂ [35]. Acetic acid that was further oxidized from acetaldehyde was exclusively found in the mesoporous TiO₂-based catalysis. The doping of vanadium did not always work positively. Typical trend by the doping of vanadium cannot be found either in mesoporous (amorphous) TiO₂ or anatase TiO₂.

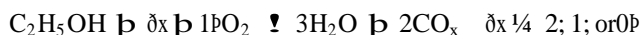
Under the illumination of visible light only, total formation rates on carbon basis followed the order (Table 1B)

$$\begin{aligned} & \text{mesoporous V} \quad \text{TiO}_2 > \text{TiO}_2 \quad \text{V=TiO}_2 \\ & > \text{V=mesoporous TiO}_2 \quad \text{mesoporous TiO}_2 \end{aligned} \quad (8)$$

Only mesoporous V–TiO₂ was superior to anatase TiO₂-based catalysts. Other mesoporous TiO₂-based catalysts were even worse than anatase TiO₂-based ones. Two groups of V + TiO₂ catalysts showed clear contrast. Ethanol dehydration proceeded on mesoporous TiO₂-based catalysts whereas exclusive dehydrogenation proceeded on anatase-TiO₂ based catalysts. For the 2-propanol decomposition, product switching from acetone (dehydrogenation) to propene (dehydration) was reported as the increase of vanadium content in V/TiO₂(anatase) catalysts at 473 K [36].

It is contradictory that the initial water formations on mesoporous V–TiO₂ and V/mesoporous TiO₂ were even faster when illuminated with visible light only than under the illumination both UV and visible light (Table 1). This may be rationalized by assuming the balance between acetaldehyde/acetic acid desorption and further consecutive oxidation reaction steps finally to form H₂O and CO₂, CO, or

carbonaceous species adsorbed



(9) catalysis again (Table 1B). The doping of both V(IV) and V(V) promoted the catalysis, however, only to mesoporous TiO₂. The total formation rates increased more by the doping of V(IV) (9.2 times, mesoporous V–TiO₂) than by V(V) doping (4.4The consumption rates ratio of O₂ and ethanol in the first 1 h were 1.8 and 1.1 for mesoporous V–TiO₂ and V/mesoporous TiO₂, respectively (Fig. 3B and C). In addition to constant dehydration reaction to form acetaldehyde and water, further breakdown reaction(s) via equation (9) may have proceeded in first 1 h on the two mesoporous TiO₂-based catalysts to form CO₂ and/or carbonaceous species (Table 1B). When water was mixed in the reactants ethanol and O₂ for the photo-oxidation reaction on Pd- and Cu-modified TiO₂(anatase) catalysts, catalytic formation of acetaldehyde was active and constant along with the minor formation of ethyleneglycol [33]. On the other hand, photocatalytic activity of pure TiO₂(anatase) and one doped with Fe became deactivated during the time course [33]. Thus, the possibility cannot be excluded in this study that initially formed water modified the mesoporous V + TiO₂ catalysts in Fig. 3B and

The effects of vanadium doping were remarkable in mesoporous TiO₂-based catalysts whereas no effects of V doping were detected in anatase TiO₂-based catalysts (Table 1B).

The vanadium local structure was reported for these V + TiO₂ catalysts [29]. Common vanadium(V) surface dispersed species (Fig. 6A) [25,27,29] was suggested for impregnated V/mesoporous TiO₂, impregnated V/TiO₂ (P-25), and sol-gel V-TiO₂ whereas V(IV) sites substituted on the Ti sites of mesoporous TiO₂ matrix for mesoporous V-TiO₂ (Fig. 6B). The relevance to ethanol photo-oxidation is first considered for data with the illumination of UV + visible light listed in Table 1A. The phase of support TiO₂, amorphous (mesoporous) or predominant anatase (P-25), was the primary factor to control the catalysis. The doping of V(V) deactivated the catalysis to form acetaldehyde, water, or acetic acid in both environments [V/mesoporous TiO₂ and V/TiO₂ (P-25)]. The doping of V(IV) maintained the total activity of mesoporous TiO₂ and directed the formation of acetic acid rather than predominant acetaldehyde over mesoporous V-TiO₂ (Fig. 6B and Table 1A). The photocatalytic activity of sol-gel V-TiO₂ catalysts in which V(IV) sites substituted on the Ti sites of TiO₂ was reported for the decompositions of methylene blue and acetaldehyde either under UV light or under visible light [6].

For the ethanol photo-oxidation with the illumination of visible light only, the phase of TiO₂ primarily controlled the

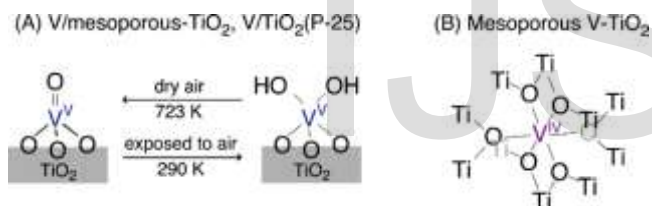


Fig. 6. Vanadium site models suggested by V K-edge XAFS study common for V/mesoporous TiO₂ and impregnated V/TiO₂ (P-25) (A) and for mesoporous V-TiO₂ (B).

times, V/mesoporous TiO₂). These catalytic trends were consistent with extension of optical absorption spectra toward visible light wavelength region for mesoporous V-TiO₂ and V/mesoporous TiO₂ (Fig. 5).

5. Conclusions

- (1) Under the illumination of UV + visible light, mesoporous V + TiO₂ catalysts generally showed faster ethanol oxidation reaction than anatase V + TiO₂ catalysts did. Major products were acetaldehyde, water, acetic acid, and carbon dioxide. Deeply oxidized acetic acid and carbon dioxide were preferably formed over the mesoporous V + TiO₂ catalysts.
- (2) Under the illumination of visible light only, mesoporous V-TiO₂ catalyst was best and superior to anatase V + TiO₂ catalysts. The phase of TiO₂ controlled the product selectivity. Ethanol dehydration and dehydrogenation proceeded on mesoporous V + TiO₂ and V + TiO₂(anatase) catalysts, respectively. V^{IV} doping was effective than V^V doping to mesoporous TiO₂, however, vanadium had no effects to anatase TiO₂.

- (3) Initial water evolution from mesoporous V-TiO₂ and V/mesoporous TiO₂ catalysts under the illumination of visible light only suggested specific catalysis utilizing the mesopore environment. Consecutive oxidation reactions to H₂O and CO_x (x = 0, 1, and 2) were suggested.
- (4) The improved photo-oxidation performance of mesoporous V-TiO₂ (and V/mesoporous TiO₂) catalyst(s) was correlated with the extension of optical absorption spectra toward visible light wavelength region.

References

- [1] P. Pichat, in: G. Ertl, H. Knözinger, J. Weitkamp (Eds.), Handbook of Heterogeneous Catalysis, vol. 4, VCH, Weinheim, 1997, pp. 2111–2122.
- [2] A. Fujishima, T.N. Rao, D.A. Tryk, J. Photochem. Photobiol. C Photochem. Rev. 1 (2000) 1–21.
- [3] M. Anpo, Bull. Chem. Soc. Jpn. 77 (2004) 1427–1442.
- [4] S.T. Martin, C.L. Morrison, M.R. Hoffmann, J. Phys. Chem. 98 (1994) 13695–13704. [5] M. Anpo, M. Takeuchi, J. Catal. 216 (2003) 505–516.
- [6] K. Iketani, R.D. Sun, M. Toki, K. Hirota, O. Yamaguchi, Mater. Sci. Eng. B 108 (2004) 187–193.
- [7] A.V. Vorontsov, V.P. Dubovitskaya, J. Catal. 221 (2004) 102–109.
- [8] J.C.S. Wu, C.H. Chen, J. Photochem. Photobiol. A Chem. 163 (2004) 509–515.
- [9] M. Sathish, B. Viswanathan, R.P. Viswanath, C.S. Gopinath, Chem. Mater. 17 (2005) 6349–6353.
- [10] J.C. D’Oliveira, C. Guillard, C. Millard, P. Pichat, J. Environ. Sci. Health A 28 (1993) 941–962.
- [11] G.K.C. Low, S.R. McEvoy, R.W. Matthews, Environ. Sci. Technol. 25 (1991) 460–467.
- [12] D.F. Ollis, Environ. Sci. Technol. 19 (1985) 480–484.
- [13] J.C. D’Oliveira, W.D.W. Jayatilake, K. Tennakone, J.M. Herrmann, P. Pichat, in: D.E. Ollis, H. Al-Ekabi (Eds.), Photocatalytic Purification and Treatment of Water and Air, Elsevier, Amsterdam, 1993, pp. 601–606.
- [14] Q. Dai, N. He, Y. Guo, C. Yuan, Chem. Lett. (1998) 1113–1114.
- [15] B. Smarsly, D. Grosso, T. Brezesinski, N. Pinna, C. Boissiere, M. Antonietti, C. Sanchez, Chem. Mater. 16 (2004) 2948–2952.
- [16] F. Schuth, Chem. Mater. 13 (2001) 3184–3195.
- [17] Y. Wang, X. Tang, L. Yin, W. Huang, Y.R. Hacoen, A. Gedanken, Adv. Mater. 12 (2000) 1183–1186.
- [18] Y. Yue, Z. Gao, Chem. Commun. (2000) 1755–1756.
- [19] Y. Wang, C. Ma, X. Sun, H. Li, J. Non-Cryst. Solids 319 (2003) 109–116.
- [20] T.Z. Ren, Z.Y. Yuan, B.L. Su, Colloids Surf. A Physicochem. Eng. Aspects 241 (2004) 67–73.
- [21] D. Zhang, L. Qi, Chem. Commun. (2005) 2735–2737.
- [22] K. Liu, M. Zhang, K. Shi, H. Fu, Mater. Lett. 59 (2005) 3308–3310.
- [23] H. Yoshitake, T. Sugihara, T. Tatsumi, Chem. Mater. 14 (2002) 1023–1029.
- [24] H. Yoshitake, T. Tatsumi, Chem. Mater. 15 (2003) 1695–1702.
- [25] B. Olthof, A. Khodakov, A.T. Bell, E. Iglesia, J. Phys. Chem. B 104 (2000) 1516–1528.
- [26] J. Haber, A. Kozłowska, R. Kozłowski, J. Catal. 102 (1986) 52–63.
- [27] G. Deo, I.E. Wachs, J. Phys. Chem. 95 (1991) 5889–5895.
- [28] A. Veijux, P. Courtine, J. Solid State Chem. 23 (1978) 93–103.
- [29] Y. Izumi, F. Kiyotaki, N. Yagi, A.M. Vlaicu, A. Nisawa, S. Fukushima, H. Yoshitake, Y. Iwasawa, J. Phys. Chem. B 109 (2005) 14884–14891.
- [30] S.J. Hwang, D. Raftery, Catal. Today 49 (1999) 353–361.
- [31] D.V. Kozlov, E.A. Paukshtis, E.N. Savinov, Appl. Catal. B Environ. 24 (2000) L7–L12.
- [32] E. Peral, J.A. Ayllon, X. Domenech, J. Peral, Catal. Today 76 (2002) 259–270.
- [33] J. Arana, J.M.D. Rodriguez, O.G. Diaz, E.T. Rendon, J.A.H. Helian, G. Colon, J.A. Navio, J.P. Pena, J. Mol. Catal. A Chem. 215 (2004) 153–160.
- [34] J. Klosek, D. Raftery, J. Phys. Chem. B 105 (2001) 2815–2819.